IEEE Access
Multidisciplinary ⋮ Rapid Review ⋮ Open Access Journal

Received December 3, 2020, accepted December 27, 2020, date of publication January 1, 2021, date of current version January 13, 2021.

Digital Object Identifier 10.1109/ACCESS.2020.3048706

Station-Keeping Control of a Hovering Over-Actuated Autonomous Underwater Vehicle Under Ocean Current Effects and Model Uncertainties in Horizontal Plane

MAI THE VU[1], HA LE NHU NGOC THANH[2], TUAN-TU HUYNH[3,4], (Member, IEEE), QUANG THANG DO[5], TON DUC DO[6], (Senior Member, IEEE), QUOC-DONG HOANG[7,8], AND TAT-HIEN LE[9,10]

[1]School of Intelligent Mechatronics Engineering, Sejong University, Seoul 143-747, South Korea
[2]HUTECH Institute of Engineering, Ho Chi Minh City University of Technology (HUTECH), Ho Chi Minh City 700000, Vietnam
[3]Department of Electrical Engineering, Yuan Ze University, Taoyuan City 32003, Taiwan, R.O.C.
[4]Department of Electrical Electronic and Mechanical Engineering, Lac Hong University, Bien Hoa 830000, Vietnam
[5]Department of Naval Architecture and Ocean Engineering, Nha Trang University, Nha Trang 650000, Vietnam
[6]Department of Robotics and Mechatronics, School Engineering and Digital Sciences, Nazarbayev University, Nur-Sultan Z05H0P9, Kazakhstan
[7]Institute of Mechanical Engineering, Vietnam Maritime University, Hai Phong 182582, Vietnam
[8]Department of Mechanical Engineering, Kyung Hee University, Seoul 130-701, South Korea
[9]Department of Naval Architecture and Marine System Engineering, Ho Chi Minh City University of Technology (HCMUT), Ho Chi Minh City, Vietnam
[10]Vietnam National University Ho Chi Minh City, Ho Chi Minh City, Vietnam

Corresponding authors: Mai The Vu (maithevu90@sejong.ac.kr), Ha Le Nhu Ngoc Thanh (hlnn.thanh@hutech.edu.vn), and Tat-Hien Le (hienlt@hcmut.edu.vn)

This research was funded by Vietnam National University Ho Chi Minh City (VNU-HCM) under grant number B2020-20-09 and in part by the Faculty Research Fund of Sejong University 2020-2021. The authors would also like to express their grateful thanks to Korea Maritime University Intelligent Robot and Automation (KIAL) Lab for their support for this study.

ABSTRACT Nowadays, underwater vehicles (UVs) are applied to various tasks such as carrying objects or maintenance of underwater structures. To carry out well these tasks, UVs should keep the position and orientation in the water to perform the specified tasks. However, the systems used in underwater operations are always under the influence of disturbance such as ocean currents and model uncertainties. In this paper, the robust station-keeping (SK) control algorithm based on a sliding mode control (SMC) theory is designed to guarantee stability and better performance of a hovering over-actuated autonomous underwater vehicle (HAUV) despite the existence of model uncertainties and ocean current disturbance in the horizontal plane (HP). Using the Lyapunov theorem, the stability of the proposed controller is demonstrated. Besides, an optimal allocation control (AC) algorithm is also designed to keep the linear position and Euler angles of the HAUV in the presence of model uncertainties as well as ocean currents and to minimize the energy consumption of the system. Finally, a series of simulations and experiments for the HAUV system is conducted to demonstrate the superior performance of the proposed method.

INDEX TERMS Over-actuated underwater vehicle, robust sliding mode controller, station-keeping control, experimental result.

I. INTRODUCTION

As the oceans contain numerous natural and mineral resources along with the depletion of resources on land, the development of resources in the ocean has been increasingly developed in recent years. With the development of the activities in the deep ocean, the UVs are becoming an active area of research, due to their various potential applications such as in maritime security, marine economy and science, marine security, marine archaeology, rescue, and military usage.

Moreover, the UVs are one of the intelligence motion platforms, which can be relied on the remote control or navigate autonomously and safely in the real marine environment and complete various missions such as pipeline inspection, environmental monitoring, underwater inspection, offshore gas and oil exploration, and exploitation, etc. [1]–[6]. There

The associate editor coordinating the review of this manuscript and approving it for publication was Zheng H. Zhu.

are many different types of the UVs for a variety of tasks that have been designed and developed, such as Autonomous Underwater Vehicles (AUV) [7], [8], Remotely Operated Vehicles (ROV) [9], [10], Underwater Gliders (UGs) [11], [12], and so on.

To carry out all the above tasks and missions, the control of the UVs faces several challenges due to some main factors such as high and couple nonlinear model, the time-varying dynamic model, model uncertainties, external disturbances by sea current and wave, unpredicted underwater currents, and so on. Some examples can be found in [13]–[15] for an overview. In recent decades, various control strategies have been proposed for improving the performances on dynamic characters of these UVs such as linear controllers [16], [17], fuzzy logic control [18], [19], SMC controllers [20], [21], predictive control algorithms [22], [23], and neural network control strategies [24].

Nowadays, dynamic positioning (DP) is applied for many purposes in ocean engineering such as drilling, underwater pipe-laying, resource exploitation, diving support, etc. The DP systems generally consist of a motion controller (MC) module and an AC module. Most DP controlled vehicles are HAUV systems with multiple thrusters, in which the AC module is adopted to distribute the specified control forces to each thruster based on mechanical or operational constraints. Using multiple active thrusters, DP control systems automatically keep the desired linear position and vehicle heading subjected to environmental disturbances and model uncertainties [25], [26]. Various control techniques have been proposed for the DP control in recent years, with many results shown in the literature. Among them are Proportional-Integral-Differential (PID) control [27], neural network control [28], adaptive control [29], fuzzy control [30], SMC [31], and so on. However, most aforementioned studies on the DP control did not mention the thruster saturation constraints into account in the DP control design. In practice, the command control input is subject to saturation constraints because of the physical limitations of the propulsion system.

Obviously, the UVs are the complex and highly nonlinear models, therefore, it is impossible and difficult to define their accurate kinematic and kinetic models. With the development of various control algorithms, the SMC is one of the control strategies that has been successfully applied to the control of the UVs due to its strong robustness to uncertain parameters and external disturbances [32]–[34]. Thus, considering the complexity of the HAUV in the HP, the SMC is selected as a DP control of the HAUV for the horizontal motion in this paper. Generally, the main goal of the overall control system of the HAUV is to provide a suitable compensation to the system, even despite the existence of the model uncertainties and external disturbance while also minimizing power consumption. Selecting wisely both the MC module and the AC module within the overall control system is an important step to achieve these objectives. Based on these, this paper describes a procedure to design a robust controller for the DP system of a HAUV subjected to the influence of the ocean current and model uncertainties. The proposed DP control system, including an MC module and an AC module, is designed. First, an MC module is designed to generate the generalized force in three degree of freedoms based on current and desired states by using the SMC law. Then, based on the generalized force, an AC module is designed by applying the Lagrange Multiplier (LM) method to distribute this generalized force amongst the thrusters of the HAUV. Numerical simulations and experimental studies are conducted to illustrate the performance of the proposed controller for SK of the HAUV under the effects of the model uncertainties and ocean currents. Both simulation and experimental results demonstrate the effectiveness and practicality of the proposed system and controller and its robustness to external disturbances.

The paper is constructed as follows. Firstly, Section 2 introduces the mathematical model of the HAUV including the effects of the ocean current. The detailed kinematics and kinetics of the HAUV are discussed in this section. Next, Section 3 explores the dynamic position system of the HAUV which has two cascade control modules: MC module and AC module. In this section, the MC module is established using robust SMC whereas we use the LM method to linear the AC module. Then, Section 4 presents some numerical simulation results and experimental results using the designed HAUV system and proposed SK system. Finally, Section 5 provides conclusions of this paper.

II. MATHEMATICAL MODEL OF A HAUV UNDER THE OCEAN CURRENT EFFECTS

A. COORDINATE SYSTEM DEFINITION

Generally, the HAUV is modeled as a body moving freely in six degree of freedoms. The dynamic model for the HAUV consists of two parts: one is a kinematic model, and the other one is a kinetic model. First, two coordinate systems are used: one coordinate is fixed to the HAUV to define its translational and rotational movements and another one is located on Earth-fixed (EF) coordinate to describe its position and orientation as illustrated in Fig. 1.

Since the HAUV moves slowly in the water, the EF coordinate system can be defined to be inertial. The EF frame $EX_EY_EZ_E$ has its origin is fixed at the water surface and three axes are respectively defined as: the Z-axis direction points down into the water while the X-axis and Y-axis directions complete a right-handed system. On the other hand, the Body-fixed (BF) frame is represented by $Bx_By_Bz_B$ with its origin located at the gravity center of the HAUV, in which the x,y,z-axes point forward, starboard side, and down the HAUV, respectively.

When the horizontal motion of the HAUV is discussed, three motions of the heave, roll, and pitch can be neglected in this study. According to SNAME [35], the motions of the HAUV in HP can be described as follows:

$\eta = \begin{bmatrix} x & y & \psi \end{bmatrix}^T \in \Re^3$: linear position and Euler angles of the HAUV in EF coordinate system.

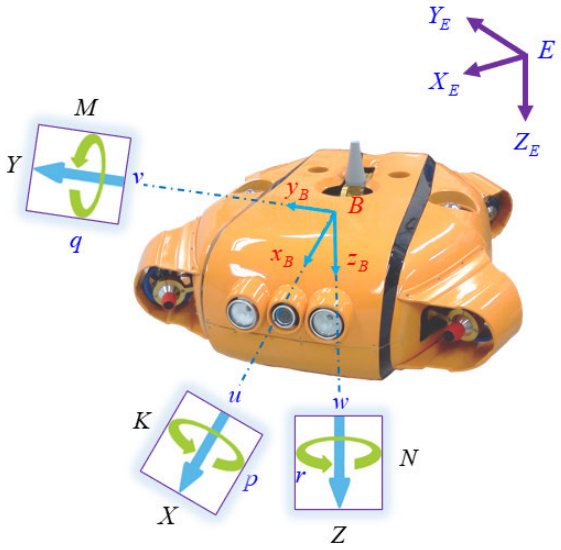

FIGURE 1. Coordinate systems of a HAUV.

$v = \begin{bmatrix} u & v & r \end{bmatrix}^T \in \Re^3$: linear and angular velocities of the HAUV in BF coordinate system.

B. HAUV KINEMATIC AND DYNAMIC MODEL IN HORIZONTAL PLANE

In this work, we concentrate on the SK problem in HP, that is the surge, sway, and yaw motions. The three degree of freedoms relationship between the BF coordinate $Bx_By_Bz_B$ and the EF coordinate $EX_EY_EZ_E$ can be described as follows:

$$\dot{\eta} = R(\eta)\, v \tag{1}$$

where, the rotation matrix $R(\eta) = R(\psi)$ is the function of the heading angle of the HAUV is defined as:

$$R(\psi) = \begin{bmatrix} \cos\psi & -\sin\psi & 0 \\ \sin\psi & \cos\psi & 0 \\ 0 & 0 & 1 \end{bmatrix}, \quad R^{-1}(\psi) = R^T(\psi) \tag{2}$$

Finally, the kinematic equations of the HAUV can be re-arranged as:

$$\begin{cases} \dot{x} = u\cos(\psi) - v\sin(\psi) \\ \dot{y} = u\sin(\psi) + v\cos(\psi) \\ \dot{\psi} = r \end{cases} \tag{3}$$

By reducing three motions of the HAUV: heave, roll, and pitch in the vertical plane motion, the horizontal motion dynamics in the BF frame can be represented as [36]:

$$M\dot{v} + C(v)v + D(v)v + G(\eta) = \tau \tag{4}$$

where $M \in \Re^{3\times3} > 0, C(v) \in \Re^{3\times3}, D(v) \in \Re^{3\times3}$ are the inertia matrix, the Centripetal and Coriolis matrix, the damping matrix of the HAUV, respectively, $G(\eta) \in \Re^3$ represents the gravitational forces, it can be assumed that gravitational forces are negligible in HP, thus, $G(\eta) = 0$, $\tau = [\tau_X,\ \tau_Y,\ \tau_N] \in \Re^3$ is the control input.

In Eq. (4), all matrices M, $C(v)$, and $D(v)$ can be expressed as:

$$\begin{aligned} M &= M_{RB} + M_A \\ &= \begin{bmatrix} m & 0 & -my_g \\ 0 & m & mx_g \\ -my_g & mx_g & I_{zz} \end{bmatrix} + \begin{bmatrix} -X_{\dot{u}} & 0 & 0 \\ 0 & -Y_{\dot{v}} & -Y_{\dot{r}} \\ 0 & -N_{\dot{v}} & -N_{\dot{r}} \end{bmatrix} \\ &= \begin{bmatrix} m - X_{\dot{u}} & 0 & -my_g \\ 0 & m - Y_{\dot{v}} & mx_g - Y_{\dot{r}} \\ -my_g & mx_g - N_{\dot{v}} & I_{zz} - N_{\dot{r}} \end{bmatrix} \end{aligned} \tag{5}$$

$$\begin{aligned} C(v) &= C_{RB}(v) + C_A(v) \\ &= \begin{bmatrix} 0 & 0 & -m(x_g r + v) \\ 0 & 0 & -m\left(y_g r - u\right) \\ m(x_g r + v) & m\left(y_g r - u\right) & 0 \end{bmatrix} \\ &\quad + \begin{bmatrix} 0 & 0 & Y_{\dot{v}} v \\ 0 & 0 & -X_{\dot{u}} u \\ -Y_{\dot{v}} v & X_{\dot{u}} u & 0 \end{bmatrix} \\ &= \begin{bmatrix} 0 & 0 & \\ 0 & 0 & \\ (Y_{\dot{v}} - m)v + mx_g r & -(m - X_{\dot{u}})\, u + my_g r & \end{bmatrix} \\ &\quad \begin{bmatrix} (Y_{\dot{v}} - m)v - mx_g r \\ (m - X_{\dot{u}})\, u - my_g r \\ 0 \end{bmatrix} \end{aligned} \tag{6}$$

$$\begin{aligned} D(v) &= D_L + D_{NL}(v) \\ &= \begin{bmatrix} -X_u & 0 & 0 \\ 0 & -Y_v & 0 \\ 0 & 0 & -N_r \end{bmatrix} \\ &\quad + \begin{bmatrix} -X_{|u|u}\,|u| & 0 & 0 \\ 0 & -Y_{|v|v}\,|v| & 0 \\ 0 & 0 & -N_{|r|r}\,|r| \end{bmatrix} \\ &= \begin{bmatrix} -X_u - X_{|u|u}|u| & 0 & 0 \\ 0 & -Y_v - Y_{|v|v}|v| & 0 \\ 0 & 0 & -N_r - N_{|r|r}|r| \end{bmatrix} \end{aligned} \tag{7}$$

Inserting Eqs. (5)-(7) into Eq. (4), the expanded form of three degree of freedoms equations of the HAUV's motion is:

$$\begin{aligned} &(m - X_{\dot{u}})\dot{u} - my_g\dot{r} + (Y_{\dot{v}} - m)vr - mx_g r^2 - X_u u \\ &\quad - X_{|u|u}\,|u|\,u = \tau_X \end{aligned} \tag{8}$$

$$\begin{aligned} &(m - Y_{\dot{v}})\dot{v} + (mx_g - Y_{\dot{r}})\dot{r} + (m - X_{\dot{u}})\, ur - my_g r^2 \\ &\quad - Y_v v - Y_{|v|v}\,|v|\,v = \tau_Y \end{aligned} \tag{9}$$

$$\begin{aligned} &-my_g\dot{u} + (mx_g - N_{\dot{v}})\dot{v} + (I_{zz} - N_{\dot{r}})\dot{r} - (Y_{\dot{v}} - m)vu \\ &\quad + mx_g ru - (m - X_{\dot{u}})\, uv + my_g rv - N_r r \\ &\quad - N_{|r|r}\,|r|\,r = \tau_N \end{aligned} \tag{10}$$

C. CONFIGURATION OF HORIZONTAL THRUSTERS

The HAUV's six degree of freedoms motions are controlled by using four horizontal thrusters and three vertical thrusters as shown in Fig. 2. However, in this paper, the motions of the HAUV are analyzed on the HP only. Thus, the simplified HAUV has four thrusters is adopted in this section.

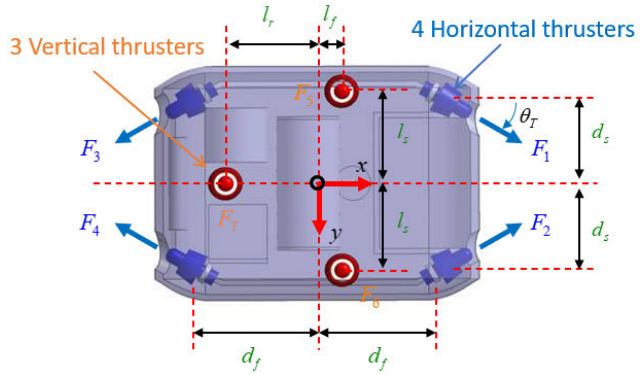

FIGURE 2. Thruster arrangement of the HAUV.

By installing these horizontal thrusters at the bow and the stern parts of the HAUV with a fixed inclined angle θ_T, the surge, sway, and yaw motions of the HAUV are operated simultaneously.

Assume $\vec{r}_i = (x_{ci}, y_{ci}, z_{ci})_{i=1,2,3,4}$ is the center point of each thruster which located on the HAUV, the moment induced by four horizontal thrusters $T_{i=1,2,3,4}$ can be respectively obtained as:

$$\begin{aligned}\vec{r}_1 \times \vec{F}_1 &= \begin{bmatrix} x_{c1} \\ y_{c1} \\ z_{c1} \end{bmatrix} \times \begin{bmatrix} F_1 \cos\theta_T \\ F_1 \sin\theta_T \\ 0 \end{bmatrix} \\ &= \begin{bmatrix} d_f \\ -d_s \\ 0 \end{bmatrix} \times \begin{bmatrix} F_1 \cos\theta_T \\ F_1 \sin\theta_T \\ 0 \end{bmatrix} \\ &= (d_f F_1 \sin\theta_T + d_s F_1 \cos\theta_T)\vec{k} \end{aligned} \tag{11}$$

$$\begin{aligned}\vec{r}_2 \times \vec{F}_2 &= \begin{bmatrix} x_{c2} \\ y_{c2} \\ z_{c2} \end{bmatrix} \times \begin{bmatrix} F_2 \cos\theta_T \\ -F_2 \sin\theta_T \\ 0 \end{bmatrix} \\ &= \begin{bmatrix} d_f \\ d_s \\ 0 \end{bmatrix} \times \begin{bmatrix} F_2 \cos\theta_T \\ -F_2 \sin\theta_T \\ 0 \end{bmatrix} \\ &= (-d_f F_2 \sin\theta_T - d_s F_2 \cos\theta_T)\vec{k} \end{aligned} \tag{12}$$

$$\begin{aligned}\vec{r}_3 \times \vec{F}_3 &= \begin{bmatrix} x_{c3} \\ y_{c3} \\ z_{c3} \end{bmatrix} \times \begin{bmatrix} -F_3 \cos\theta_T \\ F_3 \sin\theta_T \\ 0 \end{bmatrix} \\ &= \begin{bmatrix} -d_f \\ -d_s \\ 0 \end{bmatrix} \times \begin{bmatrix} -F_3 \cos\theta_T \\ F_3 \sin\theta_T \\ 0 \end{bmatrix} \\ &= (-d_f F_3 \sin\theta_T - d_s F_3 \cos\theta_T)\vec{k} \end{aligned} \tag{13}$$

$$\begin{aligned}\vec{r}_4 \times \vec{F}_4 &= \begin{bmatrix} x_{c4} \\ y_{c4} \\ z_{c4} \end{bmatrix} \times \begin{bmatrix} -F_4 \cos\theta_T \\ -F_4 \sin\theta_T \\ 0 \end{bmatrix} \\ &= \begin{bmatrix} -d_f \\ d_s \\ 0 \end{bmatrix} \times \begin{bmatrix} -F_4 \cos\theta_T \\ -F_4 \sin\theta_T \\ 0 \end{bmatrix} \\ &= (-d_f F_4 \sin\theta_T + d_s F_4 \cos\theta_T)\vec{k} \end{aligned} \tag{14}$$

where the inclined angle θ_T is set to be 30^0 in this paper.

As a result, the resultant force and moment of the propulsion system induced by four horizontal thrusters can be expressed by:

$$\begin{aligned} F_{thrust} &= F_{Tx}\vec{i} + F_{Ty}\vec{j} \\ &= (F_1 + F_2 - F_3 - F_4)\cos\theta_T \vec{i} \\ &\quad + (F_1 - F_2 + F_3 - F_4)\sin\theta_T \vec{j} \end{aligned} \tag{15}$$

$$\begin{aligned} M_{thrust} &= M_{Tz}\vec{k} \\ &= (d_f F_1 \sin\theta_T + d_s F_1 \cos\theta_T - d_f F_2 \sin\theta_T \\ &\quad - d_s F_2 \cos\theta_T - d_f F_3 \sin\theta_T - d_s F_3 \cos\theta_T \\ &\quad + d_f F_4 \sin\theta_T + d_s F_4 \cos\theta_T)\vec{k} \end{aligned} \tag{16}$$

From Eqs. (15) and (16), the horizontal thruster allocation in the matrix form can be defined as follows:

$$\tau_v = TU \tag{17}$$

$$\tau_v = \begin{bmatrix} F_{Tx} & F_{Ty} & M_{Tz} \end{bmatrix}^T \tag{18}$$

$$U = \begin{bmatrix} F_1 & F_2 & F_3 & F_4 \end{bmatrix}^T \tag{19}$$

$$T = \begin{bmatrix} \cos\theta_T & \cos\theta_T \\ \sin\theta_T & -\sin\theta_T \\ d_s\cos\theta_T + d_f\sin\theta_T & -d_s\cos\theta_T - d_f\sin\theta_T \\ -\cos\theta_T & -\cos\theta_T \\ \sin\theta_T & -\sin\theta_T \\ -d_s\cos\theta_T - d_f\sin\theta_T & d_s\cos\theta_T + d_f\sin\theta_T \end{bmatrix} \tag{20}$$

where, $\tau_v \in R^{3\times1}$ is the control forces and moments acting on the HAUV due to four horizontal thrusters, $U \in R^{4\times1}$ is the individual thruster force; and $T \in R^{3\times4}$ is the thruster configuration matrix of the propulsion system.

D. OCEAN CURRENT MODELLING

In marine engineering, the motion and stability of the HAUV are significantly affected by the ocean current. As the ocean current creates a relative speed between the fluid flow and the HAUV, thus, a hydrodynamic effect on the HAUV needs to be considered. According to Gauss-Markov process [37], the ocean current speed can be modeled as the following form:

$$\dot{V}_c + \mu_c V_c = w_c \tag{21}$$

where, $\mu_c > 0$ is a suitable constant, and w_c is Gaussian white noise. In order to limit the ocean current speed in the simulation, the bounded ocean current is set as:

$$V_{\min} \le V_c(t) \le V_{\max} \tag{22}$$

It is possible to assume that the fluid is irrotational, the ocean current speed vector in the EF coordinate is obtained as:

$$v_c^E = \begin{bmatrix} v_x & v_y & 0 \end{bmatrix}^T \tag{23}$$

where $V_c = \sqrt{v_x^2 + v_y^2}$, and the components of the ocean current in North and East directions are defined as:

$$v_x = V_c \cos\psi_c \tag{24}$$

$$v_y = V_c \sin \psi_c \tag{25}$$

where, ψ_c is the horizontal ocean current angle.

Using the rotation transformation, the relationship between the EF coordinate ocean current speed and the BF coordinate ocean current speed can be obtained as:

$$v_c^B = \begin{bmatrix} u_c^B & v_c^B & 0 \end{bmatrix}^T \tag{26}$$

$$v_c^B = diag\left[R^T(\psi)\right] v_c^E \tag{27}$$

where u_c^B and v_c^B denote the ocean current speeds in the surge and sway motions, respectively. As a result, the relative speed of the HAUV including the effects of the ocean current is given by:

$$v_r = v - v_c^B = \begin{bmatrix} u_r & v_r & r \end{bmatrix}^T \tag{28}$$

E. HAUV DYNAMIC MODEL INCLUDING OCEAN CURRENT EFFECTS

In Eq. (4), the dynamic model of the HAUV did not consider the ocean currents acting on the vehicle. First, we assume that wave-induced currents are neglected because a HAUV is deeply submerged. This section shows how to include the effects of the ocean current in the dynamic equations of the HAUV motions.

The relative speed of the three degree of freedoms- HAUV including the effects of the ocean current in Eq. (28) can be rewritten as:

$$v_r = \begin{bmatrix} u - u_c^b & v - v_c^b & r \end{bmatrix}^T \tag{29}$$

The dynamic model of the HAUV including the ocean currents expressed in the BF coordinate is in the form as:

$$\underbrace{M_{RB}\dot{v} + C_{RB}(v)v}_{Rigid-Body\ Part} + \underbrace{M_A\dot{v}_r + C_A(v_r)v_r + D(v_r)v_r}_{Hydrodynamic\ Part} + \underbrace{G(\eta)}_{Hydrostatic\ Part} = \tau \tag{30}$$

It is also possible to assume that the ocean current speed is slowly varying, which means that $\dot{v}_r \approx 0$. Thus, the dynamic model in Eq. (31) can be simplified as:

$$M\dot{v} + C_{RB}(v)v + C_A(v_r)v_r + D(v_r)v_r + G(\eta) = \tau \tag{31}$$

As a result, the kinematic and kinetic models for the HAUV including ocean current are:

$$\begin{aligned} \dot{\eta} &= J(\psi)v_r + v_c^E \\ M\dot{v} + C_{RB}(v)v + C_A(v_r)v_r + D(v_r)v_r + G(\eta) &= \tau \end{aligned} \tag{32}$$

III. DYNAMIC POSITIONING SYSTEM OF THE HAUV

To systematically handle challenges on the control performance and power of an HAUV, the whole control system consists of two cascade modules such as an MC module and an AC module as shown in Figure 3. The MC module is responsible for generating the generalized forces and moments based on current and desired states for each degree of freedom that is necessary for achieving the desired position and heading angle of the HAUV. After that, the AC module helps to distribute these generalized forces and moments to the individual thruster of the propulsion system in such a way that the overall system consumes the least power. These two modules of the whole control system are respectively explained below.

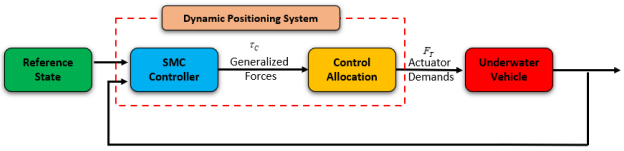

FIGURE 3. A whole control system including the MC law and AC module.

A. CONTROLLER DESIGN USING ROBUST SLIDING MODE

As the SMC is a well-know and robust control when it applies to modeling uncertainties, system parameters variation, external disturbance, the control system is designed using the SMC strategy to drive η asymptotically converge to its desired value η_d.

To simplify the complexity of designing the proposed controller, the dynamic model equation of the HAUV in the EF coordinate E-XYZ needs to be defined. For this, the following kinematic transformations are used:

$$\dot{\eta} = J(\psi)v \Leftrightarrow v = J^{-1}(\psi)\dot{\eta} \tag{33}$$

$$\ddot{\eta} = \dot{J}(\psi)v + J(\psi)\dot{v} \Leftrightarrow \dot{v} = J^{-1}(\psi)\left[\ddot{\eta} - \dot{J}(\psi)J^{-1}(\psi)\dot{\eta}\right] \tag{34}$$

By substituting Eqs. (33)-(34) into Eq. (32) and rearranging the results, the dynamic model of the HAUV in the EF coordinate can be expressed:

$$M_E\ddot{\eta} + C_E\dot{\eta} + D_E\dot{\eta} + G_E(\eta) = \tau_E \tag{35}$$

where, the transformed system matrices M_E, C_E, D_E, G_E and τ_E are obtained as:

$$\begin{aligned} M_E &= J^{-T}(\psi)MJ^{-1}(\psi) \\ C_E &= J^{-T}(\psi)\left[C(v_r) - MJ^{-1}(\psi)\dot{\eta}\right]J^{-1}(\psi) \\ D_E &= J^{-T}(\psi)D(v_r)J^{-1}(\psi) \\ G_E(\eta) &= J^{-T}(\psi)G(\eta) \\ \tau_E &= J^{-T}(\psi)\tau \end{aligned} \tag{36}$$

As a dynamical system established using Lagrangian mechanics, the dynamic equations for the HAUV expressed in Eq. (35) have some following assumptions:

Assumption 1: The inertia matrix $M_E = M_E^T > 0$ is symmetric and positive definite, and therefore: $x^T M_E x > 0$ and all eigenvalues of the matrix M_E satisfy the following condition:

$$0 < \lambda_{\min}(M_E) \leq \|M_E\| \leq \lambda_{\max}(M_E).$$

Assumption 2: Matrix $\dot{M}_E - 2C_E$ is the skew symmetric, therefore it satisfies the following formula:

$$s^T \left[\dot{M}_E - 2C_E\right] s = 0 \quad \forall\ s \in R^3,\ \eta \in R^3,\ v \in R^3.$$

Assumption 3: The matrix D_E is positive definite: $D_E > 0\ \forall\ v \in R^3$.

Assumption 4: Assume that the model uncertainties in matrices M_E, C_E, D_E, G_E of the HAUV and external disturbance F_{dis} are bounded by some known functions as follows:

$$\begin{aligned}
\left\|\tilde{M}_E\right\| &= \left\|M_E - \hat{M}_E\right\| \le \delta M_E < \infty;\\
\left\|\tilde{C}_E\right\| &= \left\|C_E - \hat{C}_E\right\| \le \delta C_E < \infty;\\
\left\|\tilde{D}_E\right\| &= \left\|D_E - \hat{D}_E\right\| \le \delta D_E < \infty;\\
\left\|\tilde{G}_E\right\| &= \left\|G_E - \hat{G}_E\right\| \le \delta G_E < \infty;\\
\left\|\tilde{F}_{dis}\right\| &= \left\|F_{dis} - \hat{F}_{dis}\right\| < \bar{F}_{dis} < \infty
\end{aligned}$$

where, $\hat{}$ and $\sim$ represent the estimated system matrices, the estimation error matrices, respectively.

Assumption 5: The following inequality is satisfied for a positively bounded diagonal matrix.

$$0 \le \lambda_{\min}(K_r)\,\|s\| \le s^T K_r \mathrm{sgn}(s); \quad K_r > 0$$

where $\lambda_{\min}$ means the smallest eigenvalue of the corresponding matrix.

Proof:

$$\begin{aligned}
&s^T K_r \mathrm{sgn}(s)\\
&= \begin{bmatrix} s_1 & s_2 & \dots & s_n \end{bmatrix}\\
&\quad \times \begin{bmatrix} K_{r_1} & 0 & 0 & 0\\ 0 & K_{r_2} & 0 & 0\\ \vdots & \vdots & \ddots & \vdots\\ 0 & 0 & 0 & K_{r_n} \end{bmatrix} \begin{bmatrix} \mathrm{sgn}(s_1)\\ \mathrm{sgn}(s_2)\\ \vdots\\ \mathrm{sgn}(s_n) \end{bmatrix}\\
&= K_{r_1} s_1 \mathrm{sgn}(s_1) + K_{r_2} s_2 \mathrm{sgn}(s_2) + \ldots + K_{r_n} s_n \mathrm{sgn}(s_n)\\
&= K_{r_1} |s_1| + K_{r_2} |s_2| + \ldots + K_{r_n} |s_n|\\
&\ge \lambda_{\min}(K_r)\,(|s_1| + |s_2| + \ldots + |s_n|)\\
&\ge \lambda_{\min}(K_r)\,\|s\| \ge 0
\end{aligned}$$

Let $\eta_d = \begin{bmatrix} x_d & y_d & \psi_d \end{bmatrix}$ be the vector of the desired position of the HAUV. Then, the tracking error is defined as:

$$e(t) = \eta_d - \eta \tag{37}$$

Differentiating with respect to time, Eq. (37) becomes:

$$\dot{e}(t) = \dot{\eta}_d - \dot{\eta} \tag{38}$$

Now, we introduce the sliding surface function as:

$$s = \dot{e} + \Lambda e = \dot{\eta}_d - \dot{\eta} + \Lambda e, \quad \Lambda > 0 \tag{39}$$

where $\Lambda > 0$ is the constant control gain which determines as a diagonal positive matrix.

According to the SMC design strategy, a control law τ for the HAUV is constructed as:

$$\tau = \tau_{eq} + \tau_{sw} \tag{40}$$

where, τ_{eq} is the equivalent term which merges the system states toward the sliding surface, and τ_{sw} is the switching term which compensates for the effect of the uncertainties and disturbances. Both the equivalent control τ_{eq} and the switching control τ_{sw} can be obtained as:

$$\begin{aligned}
\tau_{eq} &= \hat{M}_E\,(\dot{\eta}_d + \Lambda\dot{e}) + \left(\hat{C}_E + \hat{D}_E\right)(\eta_d + \Lambda e)\\
&\quad + \hat{G}_E - \hat{F}_{dis} \qquad (41)\\
\tau_{sw} &= -\beta\, sign(s) \qquad (42)
\end{aligned}$$

in which, β is the positive definite matrix of gains, and the sign function of the sliding surface is denoted by sgn(s). This sign function can be expressed as:

$$sign(s) = \begin{cases} 1 & if\ s > 0\\ 0 & if\ s = 0\\ -1 & otherwise \end{cases} \tag{43}$$

From Eqs. (41) and (42), the robust SMC law for the HAUV in Eq. (40) can be rewritten as follow:

$$\begin{aligned}
\tau = \hat{M}_E\,(\dot{\eta}_d + \Lambda\dot{e}) + \left(\hat{C}_E + \hat{D}_E\right)(\eta_d + \Lambda e) + \hat{G}_E - \hat{F}_{dis}\\
- \beta\, sign(s) \qquad (44)
\end{aligned}$$

To avoid chattering by the use of the sign function sgn in Eq. (44), we can replace the sign function with a saturating function as follows:

$$sat(\frac{s}{\phi}) = \begin{cases} \mathrm{sgn}(\frac{s}{\phi}) & if\ \left|\frac{s}{\phi}\right| > 1\\ \frac{s}{\phi} & otherwise \end{cases} \tag{45}$$

As a result, the SMC law in Eq. (44) now becomes:

$$\begin{aligned}
\tau = \hat{M}_E\,(\dot{\eta}_d + \Lambda\dot{e}) + \left(\hat{C}_E + \hat{D}_E\right)(\eta_d + \Lambda e) + \hat{G}_E - \hat{F}_{dis}\\
- \beta\, sat(s) \qquad (46)
\end{aligned}$$

Theorem 1: Let us assume that all model uncertainties and disturbance satisfy Assumption 4 and the switching control gain β is selected by Eq. (47).

$$\begin{aligned}
\lambda_{\min}(\beta) \ge \delta M_E\,\|\dot{\eta}_d + \Lambda\dot{e}\| + (\delta C_E + \delta D_E)\,\|\eta_d + \Lambda e\|\\
+ \delta G_E + \bar{F}_{dis} \qquad (47)
\end{aligned}$$

The sliding surface, s, asymptotically converges to zero if a control τ is designed by Eq. (44).

Proof: Let us consider the following Lyapunov positive candidate:

$$V = \frac{1}{2} s^T M_E s > 0 \tag{48}$$

By differentiating the proposed Lyapunov function V with respect to time, we obtain the following equation:

$$\dot{V} = \frac{1}{2} s^T \dot{M}_E s + s^T M_E \dot{s} \tag{49}$$

The first-order derivative of the sliding surface in Eq. (39) is in the form:

$$\dot{s} = \ddot{\eta} - \ddot{\eta}_d + \Lambda\dot{e} \tag{50}$$

Using Eq. (50), Eq. (49) can be rewritten as follows:

$$\dot{V} = \frac{1}{2}s^T\dot{M}_E s + s^T M_E\ddot{\eta} - s^T M_E\left(\ddot{\eta}_d - \Lambda\dot{e}\right) \quad (51)$$

The second-order derivative of η can be obtained from Eq. (35) as:

$$\ddot{\eta} = -M_E^{-1}\left[\left(C_E + D_E\right)\dot{\eta} + G_E\left(\eta\right) - \tau_E - F_{dis}\right] \quad (52)$$

Substituting Eq. (52) into Eq. (51) results in:

$$\dot{V} = \frac{1}{2}s^T\dot{M}_E s + s^T\left[-\left(C_E + D_E\right)\dot{\eta} - G_E\left(\eta\right) + \tau_E + F_{dis}\right] - s^T M_E\left(\ddot{\eta}_d - \Lambda\dot{e}\right) \quad (53)$$

From Eq. (39), we can define the first-order derivative of η as:

$$\dot{\eta} = s + \dot{\eta}_d - \Lambda e \quad (54)$$

Inserting Eq. (54) into Eq. (53) yields:

$$\begin{aligned}\dot{V} &= \frac{1}{2}s^T\dot{M}_E s + s^T\left[-\left(C_E + D_E\right)\left(s + \dot{\eta}_d - \Lambda e\right)\right. \\ &\quad \left. - G_E\left(\eta\right) + \tau_E + F_{dis}\right] - s^T M_E\left(\ddot{\eta}_d - \Lambda\dot{e}\right) \\ &= \frac{1}{2}s^T\dot{M}_E s - s^T\left[C_E s + D_E s + \left(C_E + D_E\right)\left(\dot{\eta}_d - \Lambda e\right)\right. \\ &\quad \left. + G_E\left(\eta\right) - \tau_E - F_{dis}\right] - s^T M_E\left(\ddot{\eta}_d - \Lambda\dot{e}\right) \quad (55)\end{aligned}$$

By using Assumption 2, Eq. (55) can be rewritten as:

$$\begin{aligned}\dot{V} = -s^T D_E s - s^T\left[\left(C_E + D_E\right)\left(\dot{\eta}_d - \Lambda e\right)\right. \\ \left. + G_E\left(\eta\right) - \tau_E - F_{dis}\right] - s^T M_E\left(\ddot{\eta}_d - \Lambda\dot{e}\right) \quad (56)\end{aligned}$$

Substituting the designed robust SMC law in Eq. (44) into Eq. (56) yields:

$$\begin{aligned}\dot{V} = -s^T D_E s - s^T\beta\mathrm{sgn}(s) + s^T\left[\tilde{M}_E\left(\dot{\eta}_d + \Lambda\dot{e}\right)\right. \\ \left. + \left(\tilde{C}_E + \tilde{D}_E\right)\left(\eta_d + \Lambda e\right) + \tilde{G}_E - \tilde{F}_{dis}\right] \quad (57)\end{aligned}$$

Applying Assumptions 1 and 3 and β is positive matrix, the first-order derivative of the proposed Lyapunov function V can be upper bounded as follows:

$$\begin{aligned}\dot{V} \le -\lambda_{\min} D_E\left\|s\right\|^2 - \lambda_{\min}(\beta)\left\|s\right\| \\ + \left\|s^T\left[\tilde{M}_E\left(\dot{\eta}_d + \Lambda\dot{e}\right) + \left(\tilde{C}_E + \tilde{D}_E\right)\left(\eta_d + \Lambda e\right)\right.\right. \\ \left.\left. + \tilde{G}_E - \tilde{F}_{dis}\right]\right\| \quad (58)\end{aligned}$$

By combining Assumptions 4 and 5, the inequality can be re-arranged as:

$$\begin{aligned}\dot{V} \le -\lambda_{\min}\left(D_E\right)\left\|s\right\|^2 - \lambda_{\min}(\beta)\left\|s\right\| + \left(\left\|\tilde{M}_E\right\|\left\|\dot{\eta}_d + \Lambda\dot{e}\right\|\right. \\ \left. + \left(\left\|\tilde{C}_E\right\| + \left\|\tilde{D}_E\right\|\right)\left\|\eta_d + \Lambda e\right\| + \left\|\tilde{G}_E\right\| + \left\|\tilde{F}_{dis}\right\|\right) \\ \times\left\|s\right\| \quad (59)\end{aligned}$$

$$\begin{aligned}\dot{V} \le -\lambda_{\min}\left(D_E\right)\left\|s\right\|^2 - \lambda_{\min}(\beta)\left\|s\right\| + \left(\delta M_E\left\|\dot{\eta}_d + \Lambda\dot{e}\right\|\right. \\ \left. + \left(\delta C_E + \delta D_E\right)\left\|\eta_d + \Lambda e\right\| + \delta G_E + \bar{F}_{dis}\right)\left\|s\right\| \quad (60)\end{aligned}$$

Obviously, $\dot{V} \le 0$ if the switching gains β satisfy the condition in Eq. (47). Therefore, we can conclude that the designed control system is asymptotically stable based on the Lyapunov stability.

B. LINEAR QUADRATIC CONTROL ALLOCATION USING LAGRANGE MULTIPLIERS

The AC module is responsible for delivering the forces and moments calculated by the MC law onto the available set of thrusters in a way to minimize power consumption. For the AC, the Lagrange multiplier method is used in this section. The relationship between the equivalent control input τ and the actual thruster action U can be assumed as a linear model in the form as:

$$\tau = TU \quad (61)$$

where, the matrix T is not a square matrix and has full row rank and/ or a non-trivial null space. As the result, there is an infinite number of control vectors U that satisfies Eq. (61).

To compensate for the thruster redundancy, the Moore-Penrose pseudo-inverse method is used. Firstly, a least-square cost function can be defined as:

$$\begin{aligned}U^* = \arg\min\left(U^T WU\right) \\ subject\ to\ \tau = TU \quad (62)\end{aligned}$$

where, W is a positive definite matrix weighting the thruster cost. Eq. (62) means that the AC will seek the solution that achieves the desired generalized force τ while minimizing the control effort which is represented by objective function $U^T WU$.

Next, the quadratic energy function is considered as:

$$J = \frac{1}{2}U^T WU \quad (63)$$

which can be minimized subject to

$$\tau - TU = 0 \quad (64)$$

Thus, we select the Lagrangian function, expressed as:

$$L(U, \lambda) = \frac{1}{2}U^T WU + \lambda^T(\tau - TU) \quad (65)$$

where λ denotes the Lagrange multiplier. By differentiating Eq. (65) with respect to U, we obtain the following equation:

$$\frac{\partial L}{\partial U} = WU - T^T\lambda = 0 \quad (66)$$

Using Eq. (64), Eq. (66) can be rewritten as:

$$\tau = TW^{-1}T^T\lambda \quad (67)$$

Finally, the optimal solution for the Lagrange multiplication can be obtained as follows:

$$\lambda = \left(TW^{-1}T^T\right)^{-1}\tau \quad (68)$$

Substituting Eq. (68) into Eq. (67), the generalized inverse $T_W^\dagger$ can be generated as follows:

$$T_W^\dagger = W^{-1}T^T\left(TW^1T^T\right)^{-1} \quad (69)$$

Using Eq. (69), thus, U can be calculated as:

$$U = T_W^\dagger\tau = W^{-1}T^T\left(TW^1T^T\right)^{-1}\tau \quad (70)$$

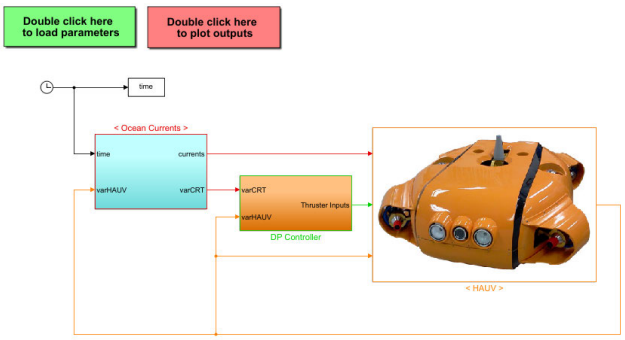

FIGURE 4. Simulation program using Matlab-Simulink.

TABLE 1. All simulation parameters.

Properties	Units	Symbols	Values
Environmental conditions			
Current velocity	m/s	v_w	0.5
Attack angle	$degree$	β_c	60
Seawater density	kg/m^3	ρ_w	1000
HAUV parameters			
Dimension	mm	$L \times B \times H$	560x750x280
Weight	kg	m	80
Gravity Point	m	X_G	(0,0,-0.06)
Buoyancy Point	m	X_B	(0,0,0)
Inertia tensor in x axis	$kg.m^2$	I_{xx}	6.9
Inertia tensor in y axis	$kg.m^2$	I_{yy}	26.1
Inertia tensor in z axis	$kg.m^2$	I_{zz}	23.2
Initial values and desired trajectory			
Initial position	$m/degree$	X_0, Y_0, ψ_0	0;0;90
Desired position	$m/degree$	X_d, Y_d, ψ_d	0;0;LOS
Parameter of SMC controller			
Parameter 1	-	$\Lambda_x, \Lambda_y, \Lambda_\psi$	7;7;10
Parameter 2	-	K_x, K_y, K_ψ	0.5;0.5;0.5

IV. RESULTS AND DISCUSSIONS

According to the established HAUV modeling and the designed control strategy, the numerical simulations for the SK control of the HAUV are presented based on the MATLAB/Simulink Software. The block diagram of this simulation program is shown in Fig. 4. The main simulation parameters and hydrodynamic coefficients of the HAUV are shown in Table 1 and Table 2, respectively.

A. SK CONTROL OF THE HAUV IN THE HORIZONTAL PLANE

To validate the robustness of the designed controller to eliminate the ocean current disturbances and the model uncertainties, the simulation for a SK control of the three degree of freedoms-HAUV on the HP is carried out. In this simulation, we assume that a random value between -35% and 35% is applied as the model uncertainties of the HAUV operating under the water such as in the mass, the inertia tensor, and the hydrodynamic coefficients. Moreover, Fig. 5 shows the average velocity and the direction angle of the ocean current during this simulation. In this case, it is possible to assume

TABLE 2. Hydrodynamic coefficients.

Parameters	Units	Value	Description
$X_{\dot{u}}$	kg	-29	Added mass
X_u	kg/s	-72	Linear damping
$X_{u\|u\|}$	kg/m	-227.18	Axial drag
$Y_{\dot{v}}$	kg	-30	Added mass
$Y_{\dot{r}}$	$kg.m$	1.93	Added mass
Y_v	kg/s	-77	Linear damping
$Y_{v\|v\|}$	kg/m	-405.41	Cross-flow drag
$N_{\dot{v}}$	kg	1.93	Added mass
$N_{\dot{r}}$	$kg.m$	-3.3	Added mass
N_r	$kg.m/s$	-30	Linear damping
$N_{r\|r\|}$	$kg.m$	-12.937	Cross-flow drag

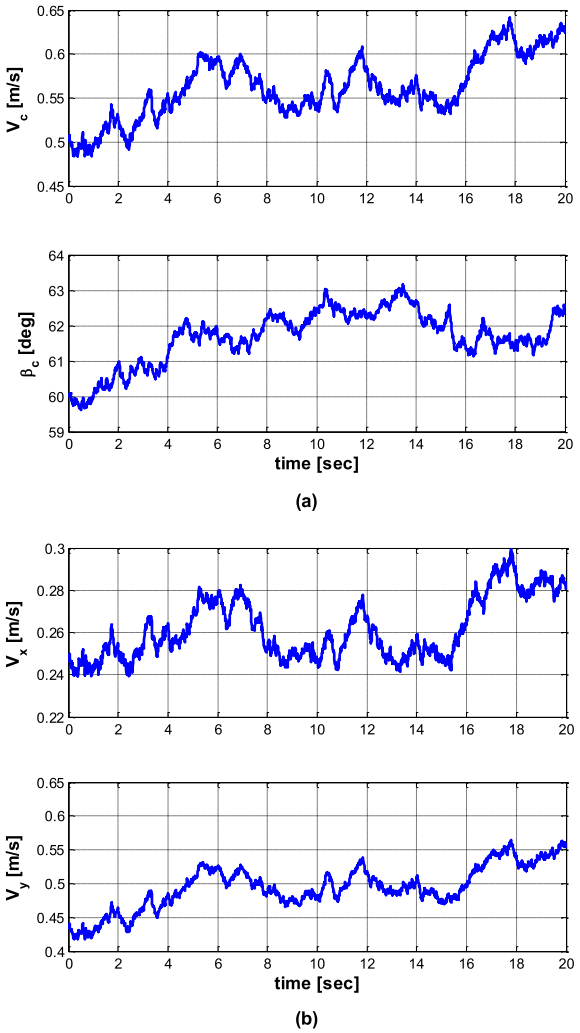

FIGURE 5. Ocean current form applying to SK control simulation of HAUV in a horizontal plane: (a) ocean current parameters; (b) ocean current vector w.r.t Earth fixed coordinate EXYZ.

that the ocean currents are irrotational fluid, slowly varying with respect to the time, and thus the first Gauss-Markov process is used to simulate the ocean currents expressed in

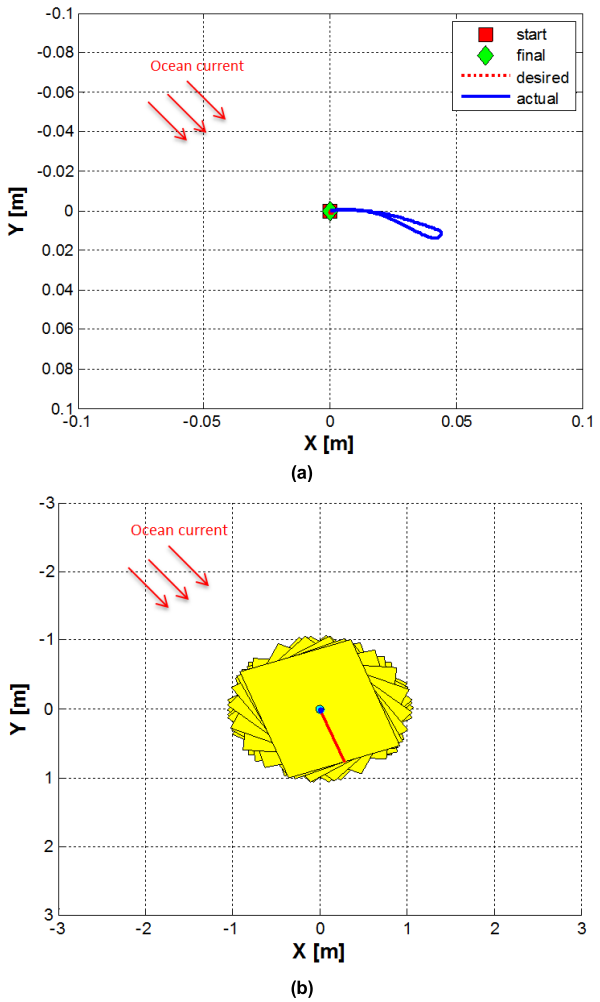

FIGURE 6. SK control simulation results of HAUV using SMC controller in horizontal plane: (a) 2D trajectory of HAUV; (b) 2D shape diagram of HAUV.

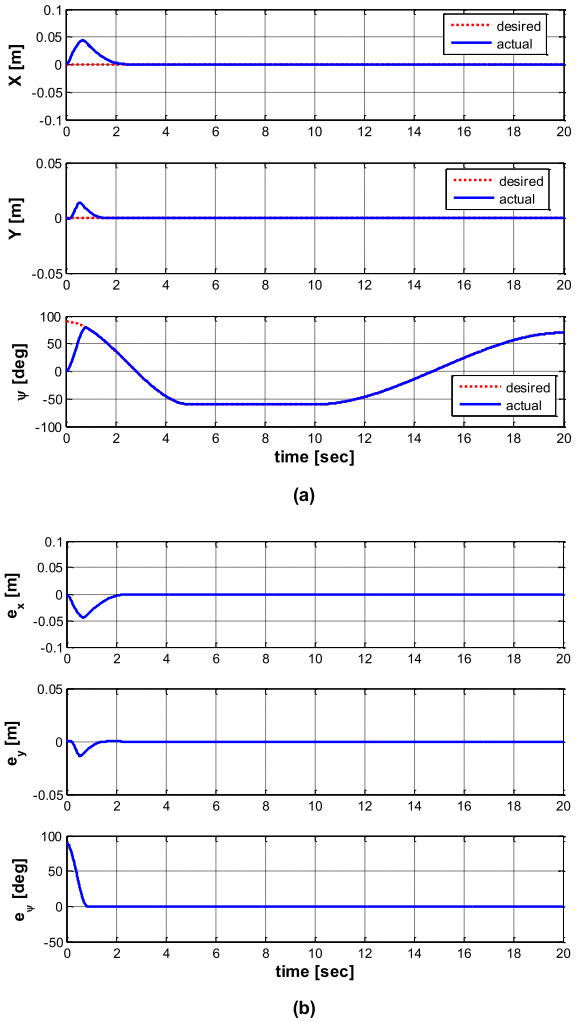

FIGURE 7. State variables of HAUV in horizontal plane: (a) position and heading angle; (b) errors of state variables.

two dimensions model. The behaviors of the ocean currents are shown in Fig. 5a with an average velocity of the ocean current is 0.5 m / s (about 1 knot) and the angle of attack is 60°. Meanwhile, the velocity vector of the ocean current expressed in the EF coordinate system EXYZ is shown in Fig. 5b.

In this simulation, the HAUV is requested to stay at point (0, 0) [m] while tracking the specified heading angle in a case where the average velocity of the ocean current is 0.5m/s and initial direction angle of the average ocean current is 60°. The trajectory of the HAUV in horizontal motion can be observed in Fig. 6. As shown in Fig. 6a, the HAUV is taken out of its set point in the x and y coordinates about 4 cm along the direction of the ocean current due to the effects of the ocean current, however, the HAUV rapidly converges to the initial position (0,0) [m] thanks to the designed controller. Fig. 6b shows that the HAUV in the HP rotates according to the target heading angle while keeping the initial position during the simulation.

Fig. 7a shows the linear position x, y and heading angle ψ of the HAUV with the changing time. As can be seen from the results, the HAUV maintains the initial position (0, 0) [m], and the heading angle follows the desired heading angle of 90 ° from the initial heading angle of 0 °. At the beginning of the simulation, a slight push appears in the x and y-directions due to the effects of the ocean current, however, the HAUV quickly moves back to the initial position thanks to the designed robust SMC controller. Also, it is observed that the heading angle of the HAUV is well driven with the lapse of the time despite the existence of a big error between the initial and the designed heading angles whereas the linear position (0, 0) of the HAUV kept without large error. Fig. 7b shows the errors of the state variables of the HAUV during the simulation.

Finally, to track the desired heading angle while keeping the initial linear position of the HAUV, the forces and moments of the control obtained through the robust SMC designed in the previous section are shown in Fig. 8a. Besides, according to the designed AC algorithm, the thruster forces generated by the four horizontal thrusters are obtained to optimize the energy consumption while satisfying the control

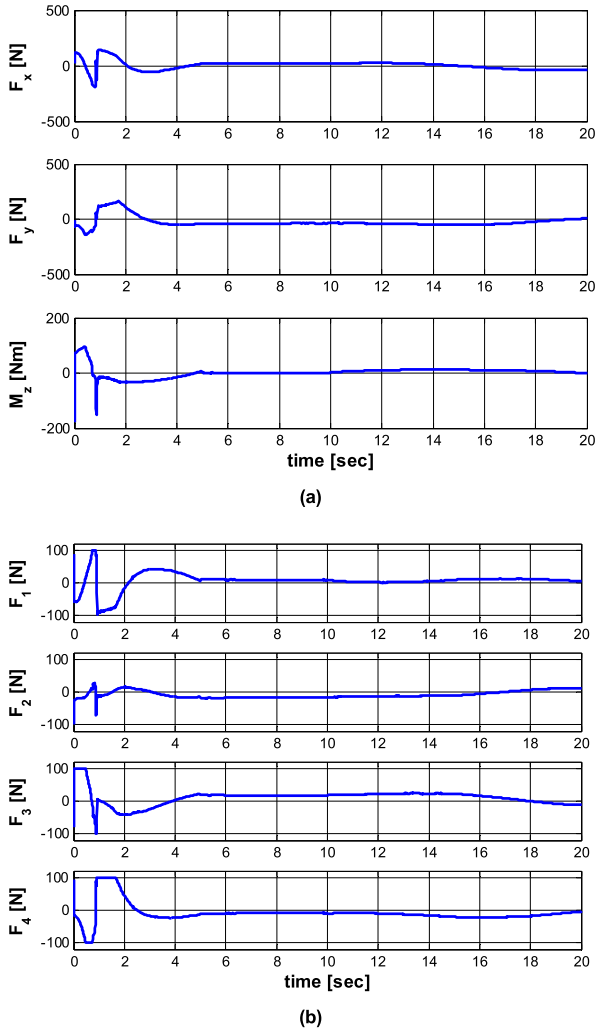

FIGURE 8. Control inputs and thruster forces in horizontal plane: (a) control inputs of controller; (b) horizontal thruster forces.

input as shown in Fig. 8b. It can be also seen that the thruster force produced in individual thrusters is operated within the limit range from −100N to 100N of the predefined thrust according to the real technical specifications of each thruster.

B. EXPERIMENTAL RESULTS AND DISCUSSION

In this section, we present a SK experiment of the HAUV to confirm the performance of the proposed control system as shown in Fig. 9.

Firstly, in order to confirm the performance of the SMC that is robust to the effects of the ocean current and model uncertainties proposed in this study, an ocean current disturbance is applied to the HAUV in a specific direction from the outside. The effects of the tidal current with the velocity of about 1 knot and the direction angle of 90° on the HAUV are assessed. Then, a number of unknown masses are attached to the hull of the HAUV to simulate the model uncertainties to the HAUV system.

Under the setting environments, the first experiment is conducted to stabilize the HAUV satisfying the constraints

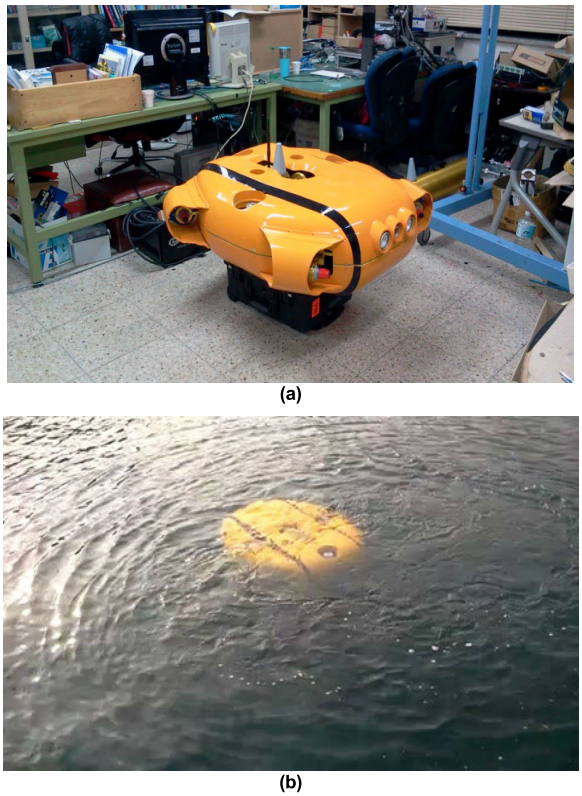

FIGURE 9. SK control experiments of HAUV in horizontal plane: (a) HAUV platform; (b) conducting experiments of HAUV.

of keeping a specific position at (0,0) m and of following the desired heading angle of 120 degrees in 90 seconds under ocean current disturbance and model uncertainties as shown in Fig. 10. In this experiment, the effectiveness of the robust SMC control in unknown perturbations of the HAUV system is verified in this experiment by comparing it with the PD control method. Fig. 10a shows the result of the heading angle control of the HAUV. As shown in this figure, in the case of the ocean current disturbances and model uncertainties, the maximum error of about ±5° is included in the heading control when using the PD controller to perform the SK control of the HAUV. On the other hand, the heading angle control of the HAUV through the SMC is much better. It is observed that the control error is maintained within ±1° during the experiment.

Fig. 10b shows the 2D trajectory of the HAUV in the HP. As shown in the results, it can be seen that when the PD control is applied, the position of the HAUV is deviated from the target position by at least 1m in the direction of the ocean current, while its position is maintained within about ±0.2m when the SMC is used. According to these results, we found that using the SMC algorithm is better than the PD in the SK control of the HAUV under the model uncertainties and the effects of the ocean current. Lastly, Fig. 10c shows the thruster forces generated by the four horizontal thrusters to satisfy the control input obtained through an AC algorithm during the experiment.

As mentioned in the first experiment, Fig. 10c shows the result of adding the saturation condition to the actual thrusters

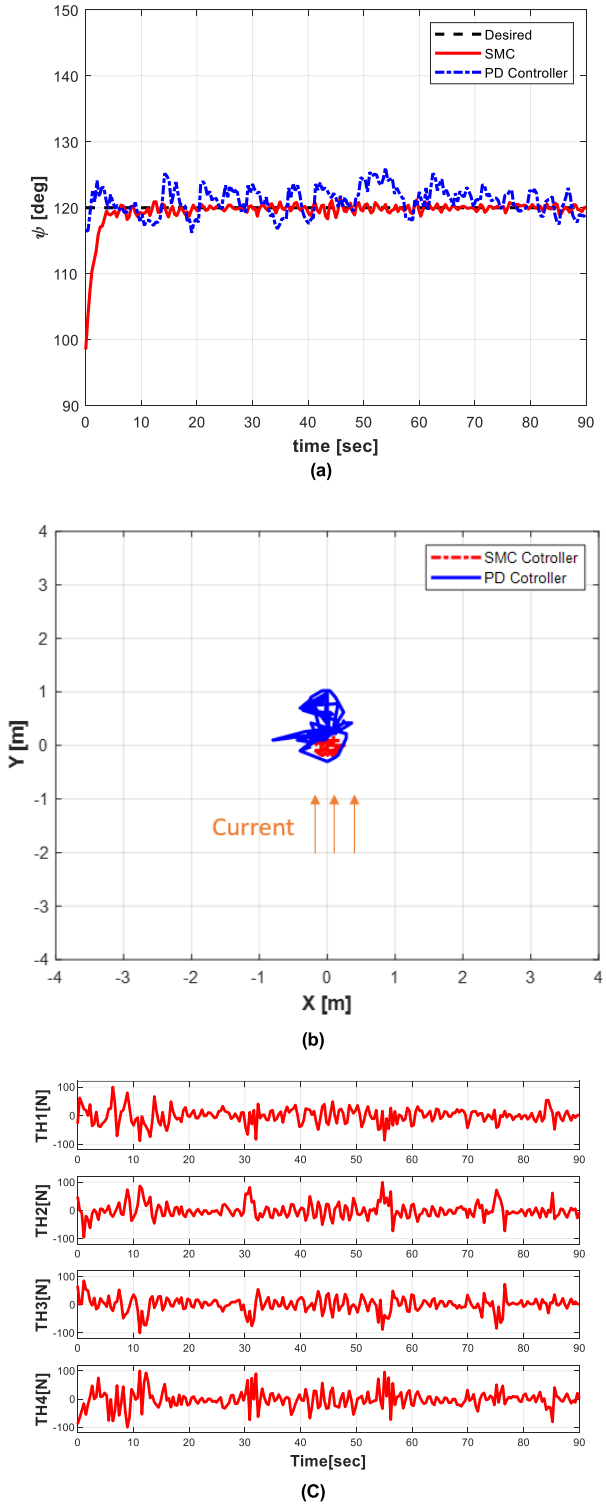

FIGURE 10. Experiment results of SK control using SMC controller in horizontal plane: (a) heading angle of HAUV; (b) 2D trajectory of HAUV in horizontal plane; (c) four horizontal thruster forces.

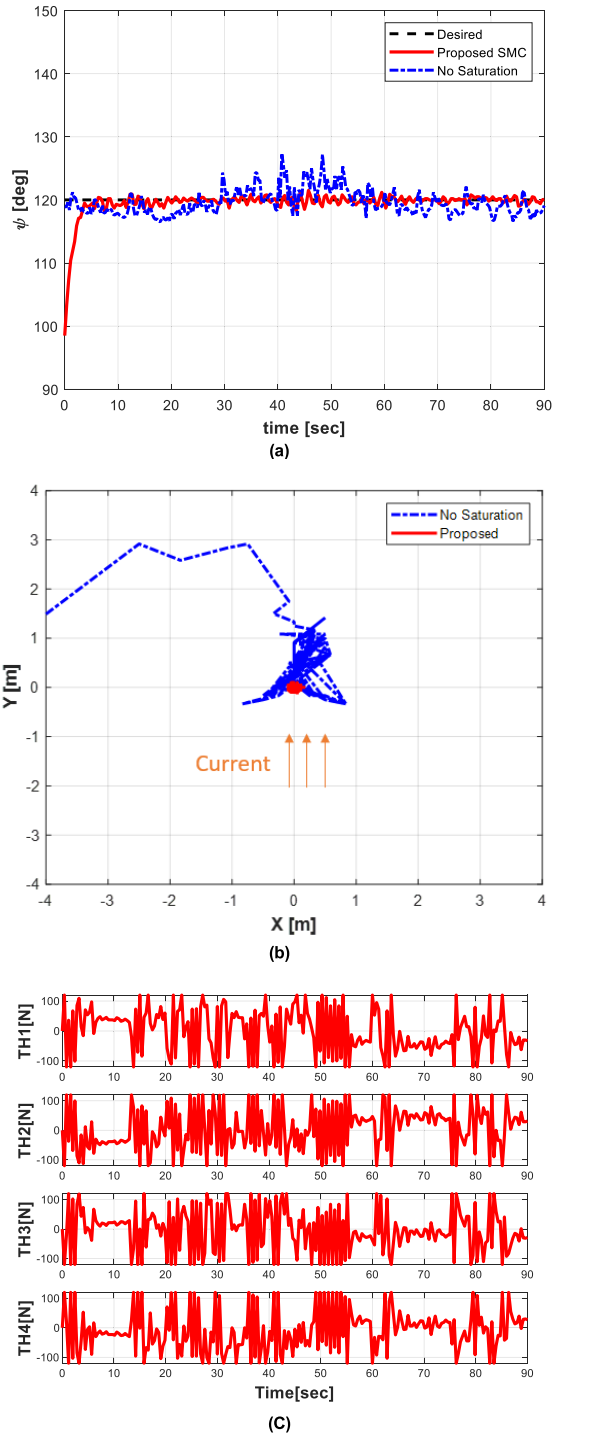

FIGURE 11. Experiment results of SK control without actuator saturation: (a) heading angle of HAUV; (b) 2D trajectory of HAUV in horizontal plane; (c) four horizontal thruster forces.

after determining the control input in the SMC case. To verify the optimization of the proposed AC algorithm in this study, the second experiment is performed to compare with the one in the first experiment as shown in Fig. 11. As shown in Figs. 11a and b, in the case of without considering the saturation of the thruster, the heading angle of the HAUV shows an error of up to 10°, and the position of the HAUV in the HP shows the result of diverging without maintaining the target position. This is because the driving saturation phenomenon of the thruster forces continuously occurs, which lowers the control performance as shown in Fig. 11c. Therefore, through such

an experiment, the effectiveness of the optimal AC algorithm proposed in this study can be confirmed.

V. CONCLUSION

In this paper, the design of the SK control, and the experimental implementation of a HAUV platform are performed. Using four horizontal thrusters and three vertical thrusters for the propulsion system, the hovering operation and maneuverability of the HAUV are more efficiency and high capacity. Firstly, the kinematic and kinetic equations of the HAUV under the model uncertainties and the ocean current disturbances are established. Next, a SK control scheme is proposed based on an MC module and an optimal AC module. To do so, the SMC controller is used to figure out the appropriate forces and moments to keep the HAUV at the fixed linear position and the desired heading angle. Then, an AC module allocates these forces and moments to individual thrusters of the HAUV as the thruster commands by using the LM method. The stability of the designed controller has been proved thoroughly based on the Lyapunov criteria. In order to demonstrate the performance of the proposed controller and its robustness to the model uncertainties and ocean current disturbance, the numerical simulation and experimental tests have been carried out. The simulation results verified the superior performance of the proposed algorithm under the uncertainties parameters and the ocean current disturbances. Especially, the results of the field experiments verify the feasibility of the HAUV control system in the HP motion.

REFERENCES

[1] M. T. Vu, H.-S. Choi, J.-Y. Kim, and N. H. Tran, "A study on an underwater tracked vehicle with a ladder trencher," *Ocean Eng.*, vol. 127, pp. 90–102, Nov. 2016.

[2] Y. Wang, L. Gu, M. Gao, and K. Zhu, "Multivariable output feedback adaptive terminal sliding mode control for underwater vehicles," *Asian J. Control*, vol. 18, no. 1, pp. 247–265, Jan. 2016.

[3] M. T. Vu, H.-S. Choi, N. D. Nguyen, and S.-K. Kim, "Analytical design of an underwater construction robot on the slope with an up-cutting mode operation of a cutter bar," *Appl. Ocean Res.*, vol. 86, pp. 289–309, May 2019.

[4] L. Qiao, B. Yi, D. Wu, and W. Zhang, "Design of three exponentially convergent robust controllers for the trajectory tracking of autonomous underwater vehicles," *Ocean Eng.*, vol. 134, pp. 157–172, Apr. 2017.

[5] K. Shojaei and M. M. Arefi, "On the neuro-adaptive feedback linearising control of underactuated autonomous underwater vehicles in three-dimensional space," *IET Control Theory Appl.*, vol. 9, no. 8, pp. 246–258, 2015.

[6] M. T. Vu, H.-S. Choi, D. H. Ji, S.-K. Jeong, and J.-Y. Kim, "A study on an up-milling rock crushing tool operation of an underwater tracked vehicle," *Proc. Inst. Mech. Eng. M, J. Eng. Maritime Environ.*, vol. 233, no. 1, pp. 283–300, Feb. 2019.

[7] M. T. Vu, H.-S. Choi, T. Q. M. Nhat, N. D. Nguyen, S.-D. Lee, T.-H. Le, and J. Sur, "Docking assessment algorithm for autonomous underwater vehicles," *Appl. Ocean Res.*, vol. 100, Jul. 2020, Art. no. 102180.

[8] H. Cho, S.-K. Jeong, D.-H. Ji, N.-H. Tran, M. T. Vu, and H.-S. Choi, "Study on control system of integrated unmanned surface vehicle and underwater vehicle," *Sensors*, vol. 20, no. 9, p. 2633, May 2020.

[9] M. T. Vu, M. Van, D. H. P. Bui, Q. T. Do, T.-T. Huynh, S.-D. Lee, and H.-S. Choi, "Study on dynamic behavior of unmanned surface vehicle-linked unmanned underwater vehicle system for underwater exploration," *Sensors*, vol. 20, no. 5, p. 1329, Feb. 2020.

[10] J. I. Kang, H. S. Choi, M. T. Vu, N. D. Nguyen, D. H. Ji, and J. Y. Kim, "Experimental study of dynamic stability of underwater vehicle-manipulator system using zero moment point," *J. Mar. Sci. Technol.-Taiwan.*, vol. 25, no. 6, pp. 767–774, 2017.

[11] C. Deutsch, J. Kuttenkeuler, and T. Melin, "Glider performance analysis and intermediate-fidelity modelling of underwater vehicles," *Ocean Eng.*, vol. 210, Aug. 2020, Art. no. 107567.

[12] H. Wu, W. Niu, S. Wang, and S. Yan, "Prediction method of permissible error ranges of control parameters for underwater gliders under given operation accuracy," *Appl. Ocean Res.*, vol. 103, Oct. 2020, Art. no. 102153.

[13] G. Antonelli, T. I. Fossen, and D. R. Yoerger, "Underwater robotics," in *Springer Handbook of Robotics*. Berlin, Germany: Springer, 2008, pp. 987–100.

[14] M. The Vu, H.-S. Choi, J. Kang, D.-H. Ji, and S.-K. Jeong, "A study on hovering motion of the underwater vehicle with umbilical cable," *Ocean Eng.*, vol. 135, pp. 137–157, May 2017.

[15] D. W. Jung, S. M. Hong, J. H. Lee, H. J. Cho, H. S. Choi, and M. T. Vu, "A study on unmanned surface vehicle combined with remotely operated vehicle system," *Proc. Eng. Technol. Innov.*, vol. 9, pp. 17–24, Jul. 2019.

[16] J. A. Farrell, S. Pang, W. Li, and R. M. Arrieta, "Biologically inspired chemical plume tracing on an autonomous underwater vehicle," in *Proc. IEEE Int. Conf. Syst., Man Cybern.*, Hague, The Netherlands, Oct. 2004, pp. 10–13.

[17] Ö. Yildiz, R.B. Gökalp, and A.E. Yilmaz, "A review on motion control of the underwater vehicles," in *Proc. Int. Conf. Electr. Electron. Eng. (ELECO)*, Bursa, Turkey, Nov. 2009, pp. 5–8.

[18] S. W. Jun and H. J. Lee, "Design of TS fuzzy-model-based controller for depth control of autonomous underwater vehicles with parametric uncertainties," in *Proc. 11th Int. Conf. Control, Automat. Syst.*, Gyeonggi-do, South Korea, Oct. 2011, pp. 26–29.

[19] H. Dahmani, M. Chadli, A. Rabhi, and A. El Hajjaji, "Road curvature estimation for vehicle lane departure detection using a robust Takagi–Sugeno fuzzy observer," *Vehicle Syst. Dyn.*, vol. 51, no. 5, pp. 581–599, May 2013.

[20] M. Zeinali and L. Notash, "Adaptive sliding mode control with uncertainty estimator for robot manipulators," *Mechanism Mach. Theory*, vol. 45, no. 1, pp. 80–90, Jan. 2010.

[21] M. T. Vu, C. H. Sik, T. Q. M. Nhat, and D. W. Jung, "Designing optimal trajectories and tracking controller for unmanned underwater vehicles," in *Recent Advances in Electrical Engineering and Related Sciences: Theory and Application—AETA* (Lecture Notes in Electrical Engineering), vol. 465. Cham, Switzerland: Springer, 2017.

[22] L. Medagoda and S. B. Williams, "Model predictive control of an autonomous underwater vehicle in an *in situ* estimated water current profile," in *Proc. Oceans Yeosu*, Yeosu, South Korea, May 2012, pp. 21–24.

[23] L. V. Steenson, "Experimentally verified model predictive control of a hover-capable AUV," Ph.D. dissertation, Dept. Eng. Environ., Univ. Southampton, Southampton, U.K., 2013.

[24] N. Kumar, V. Panwar, N. Sukavanam, S. P. Sharma, and J. H. Borm, "Neural network-based nonlinear tracking control of kinematically redundant robot manipulators," *Math. Comput. Model.*, vol. 53, nos. 9–10, pp. 1889–1901, May 2011.

[25] A. J. Sørensen, "A survey of dynamic positioning control systems," *Annu. Rev. Control*, vol. 35, no. 1, pp. 123–136, Apr. 2011.

[26] T. I. Fossen and J. P. Strand, "Passive nonlinear observer design for ships using Lyapunov methods: Full-scale experiments with a supply vessel," *Automatica*, vol. 35, no. 1, pp. 3–16, Jan. 1999.

[27] P. Martin and R. Katebi, "Multivariable PID tuning of dynamic ship positioning control systems," *J. Mar. Eng. Technol.*, vol. 4, no. 2, pp. 11–24, Jan. 2005.

[28] J. Du, Y. Yang, D. Wang, and C. Guo, "A robust adaptive neural networks controller for maritime dynamic positioning system," *Neurocomputing*, vol. 110, pp. 128–136, Jun. 2013.

[29] X. Lin, J. Nie, Y. Jiao, K. Liang, and H. Li, "Nonlinear adaptive fuzzy output-feedback controller design for dynamic positioning system of ships," *Ocean Eng.*, vol. 158, pp. 186–195, Jun. 2018.

[30] X. Hu, J. Du, and J. Shi, "Adaptive fuzzy controller design for dynamic positioning system of vessels," *Appl. Ocean Res.*, vol. 53, pp. 46–53, Oct. 2015.

[31] E. A. Tannuri, A. C. Agostinho, H. M. Morishita, and L. Moratelli, "Dynamic positioning systems: An experimental analysis of sliding mode control," *Control Eng. Pract.*, vol. 18, no. 10, pp. 1121–1132, Oct. 2010.

[32] H. L. N. N. Thanh, M. T. Vu, N. X. Mung, N. P. Nguyen, and N. T. Phuong, "Perturbation observer-based robust control using a multiple sliding surfaces for nonlinear systems with influences of matched and unmatched uncertainties," *Mathematics*, vol. 8, no. 8, p. 1371, Aug. 2020.
[33] M. T. Vu, H. S. Choi, J. I. Kang, D. H. Ji, and H. Joong, "Energy efficient trajectory design for the underwater vehicle with bounded inputs using the global optimal sliding mode control," *J. Mar. Sci. Technol.-Taiwan.*, vol. 25, pp. 705–714, Dec. 2017.
[34] N. Ali, I. Tawiah, and W. Zhang, "Finite-time extended state observer based nonsingular fast terminal sliding mode control of autonomous underwater vehicles," *Ocean Eng.*, vol. 218, Dec. 2020, Art. no. 108179.
[35] S. H. Subcommittee, "Nomenclature for treating the motion of a submerged body through a fluid," in *Proc. Amer. Towing Tank Conf.*, New York, NY, USA, Sep. 1950, pp. 11–14.
[36] T. I. Fossen, *Guidance and Control of Ocean Vehicles*. New York, NY, USA: Wiley, 1994.
[37] T. I. Fossen, *Handbook of Marine Craft Hydrodynamics and Motion Control*. Hoboken, NJ, USA: Wiley, 2011.

MAI THE VU received the B.S. degree in naval architecture and marine engineering from the Ho Chi Minh City University of Technology, Vietnam, in 2013, and the Ph.D. degree from the Department of Convergence Study on the Ocean Science and Technology, Korea Maritime and Ocean University, South Korea, in 2019. He is currently an Assistant Professor with the Department of Unmanned Vehicle Engineering, Sejong University, South Korea. His research interests include underwater vehicles and robotics, multi-body dynamic modeling, linear and nonlinear control, trajectory tracking, path planning, obstacle avoidance, and intelligent navigation.

HA LE NHU NGOC THANH received the B.S. degree in mechanical engineering from the HCMC University of Technology and Education, in 2011, the M.S. degree from the HCMC University of Technology, Vietnam, in 2015, and the Ph.D. degree from the Mechanical and Aerospace Engineering, Sejong University, Seoul, South Korea, in 2019. He is currently a Lecturer with the Vietnam–Korea Institution of Technology, Ho Chi Minh City University of Technology (HUTECH), Ho Chi Minh City, Vietnam. His research interests include nonlinear control, mechatronics and robotics. He received an Outstanding Research Award in Sejong University in 2019. He also serves as a Guest Editor for *Sensor* journal (MDPI), and *Applied Sciences* journal (MDPI).

TUAN-TU HUYNH (Member, IEEE) was born in Ho Chi Minh City, Vietnam, in 1982. He received the B.S. degree in electrical and electronics from the Department of Electrical & Electronics Engineering, Ho Chi Minh University of Technology and Education, Vietnam, in 2005, the M.S. degree in Automation from the Ho Chi Minh City University of Transport, Vietnam, in 2010, and the Ph.D. degree in electrical engineering from Yuan Ze University, Taoyuan City, Taiwan, in 2018. He is currently a Research Fellow with the Department of Electrical Engineering, Yuan Ze University, Chungli, Taiwan. He is also a Lecturer with the Faculty of Mechatronics and Electronics, Lac Hong University, Vietnam. His research interests include MCDM, fuzzy logic control, neural networks, cerebellar model articulation controller, brain emotional learning-based intelligent controller, deep learning, and intelligent control systems.

QUANG THANG DO received the B.S. degree in naval architecture and ocean engineering from Nha Trang University, Vietnam, in 2009, and the M.Sc. and Ph.D. degrees from the School of Naval Architecture and Ocean Engineering, University of Ulsan, South Korea, in 2016 and 2019, respectively. He is currently an Assistant Professor with the Department of Naval Architecture and Ocean Engineering, Nha Trang University. His research interests include ocean engineering, structural engineering, submarine structures, nonlinear static and dynamic structural analysis, ultimate strength and damage assessments of steel-plated, cylindrical and thin-walled shell structures, accidental loads on offshore structures, structural impact and ultimate strength tests, and advanced and optimal structural design for stiffened cylinder structures.

TON DUC DO (Senior Member, IEEE) received the B.S. and M.S. degrees in electrical engineering from the Hanoi University of Science and Technology, Hanoi, Vietnam, in 2007 and 2009, respectively, and the Ph.D. degree in electrical engineering from Dongguk University, Seoul, South Korea, in 2014. From 2008 to 2009, he worked with the Division of Electrical Engineering, Thuy Loi University, Vietnam, as a Lecturer. He was with the Division of Electronics and Electrical Engineering, Dongguk University, as a Postdoctoral Researcher, in 2014. He was also a Senior Researcher with the Pioneer Research Center for Controlling Dementia by Converging Technology, Gyeongsang National University, South Korea, from May 2014 to August 2015. Since September 2015, he has been an Assistant Professor with the Department of Robotics and Mechatronics, Nazarbayev University, Kazakhstan. His research interests include advanced control system theories, electric machine drives, renewable energy conversion systems, uninterruptible power supplies, electromagnetic actuator systems, targeted drug delivery systems, and nanorobots. He received the Best Research Award from Dongguk University in 2014. He was also the Lead Guest Editor for special issue for the special issue of Mathematical Problems in Engineering on *Advanced Control Methods for Systems with Fast-Varying Disturbances and Applications*. He is also an Associate Editor of IEEE Access.

QUOC-DONG HOANG received the B.E. and M.S. degrees in mechanical engineering from Vietnam Maritime University, Haiphong, Vietnam, in 2010 and 2014, respectively. His Ph.D. dissertation in Mechanical Engineering is completed in Kyung Hee University, Yongin, South Korea, in 2020. His research interests include nonlinear control, artificial intelligent control, and mechatronics. Since 2010, he has been held research and teaching position in the Institute of Mechanical Engineering, Vietnam Maritime University.

TAT-HIEN LE was born in 1981. He received the bachelor's degree in naval architecture and marine engineering from the Ho Chi Minh City University of Technology, Vietnam National University Ho Chi Minh City (VNU-HCM), Vietnam, in 2004, and the M.Sc. and Ph.D. degrees from Pukyong National University, South Korea, in 2006 and 2009, respectively. His research interests include ocean engineering, structural engineering, and submarine structures.